

## Observation of large parity-change-induced dispersion in triangular-lattice photonic crystal waveguides using phase sensitive techniques

Jiandong Huang,<sup>a)</sup> Charles M. Reinke, Aliakbar Jafarpour, Babak Momeni, Mohammad Soltani, and Ali Adibi  
*School of Electrical and Computer Engineering, Georgia Institute of Technology, Atlanta, Georgia 30332-0259*

(Received 8 March 2005; accepted 29 December 2005; published online 15 February 2006)

We experimentally studied W1 triangular-lattice photonic crystal waveguides (PCWs) fabricated on semiconductor-on-insulator substrates using phase-sensitive lock-in techniques. In addition to the improved signal-to-noise ratio for power transmission measurements, we observed two large group delay peaks at frequencies corresponding to the photonic mode gap and parity changes of Bloch modes inside the PCWs. © 2006 American Institute of Physics. [DOI: 10.1063/1.2174098]

Photonic crystals (PCs) have inspired much interest with their unique ability to control light propagation and emission through the photonic band gap (PBG).<sup>1-3</sup> Planar two-dimensional PCs are excellent candidates for integrating the functions of waveguides, resonators, filters, couplers, etc., onto a single chip to form small footprint photonic circuits.<sup>4</sup> Due to their large PBGs, triangular-lattice PC waveguides (PCWs), which are formed by removing one row of air holes (W1) from the otherwise perfect PC lattice, are attractive for forming the backbone of such photonic circuits.<sup>5</sup> Currently, however, the calibration and experimental studies of these structures are often hindered by the low signal-to-noise ratio (SNR) of the measurements. Design efforts have been made to improve the SNR by increasing the light coupling efficiency in and out of the PCWs, for example, by using adiabatic tapers.<sup>6</sup> These designs decrease the overall insertion loss of the PCW circuits, but are limited by available processing technologies and can possibly distort the propagation properties of the modes of the PCWs. Additionally, it is still a challenge to measure the dispersion of PCWs at optical frequencies,<sup>7</sup> which is a critical parameter for designing high-speed optical circuits.

In this letter, we report the experimental observation of large parity-change-induced dispersion in triangular-lattice PCWs using phase-sensitive techniques. By using a lock-in amplifier, we can improve the SNR of the power transmission measurements by at least one order of magnitude, while at the same time making direct correlations between features in the group delay spectra (obtained from phase measurements) and the complex transmission properties (i.e., amplitude and phase) of the PCWs. From using this technique, we also report the observation of large group delays close to the mode gap of this PCWs.

The schematic experimental setup is shown in Fig. 1(a): The infrared (IR) lasers (a multiplexed series of four lasers from Agilent Technologies Inc., tunable from 1260 nm to 1640 nm with  $\sim 100$  kHz linewidth) are triggered by a common square-wave modulation signal at frequency  $f_M=20$  kHz, while the average output power was kept constant at 0.5 mW. A lock-in amplifier (SR 830 from Stanford Research Systems) is also synchronized to the same trigger signal to allow for phase measurements of better than

$1^\circ$  (0.017 rad) resolution. The laser beam was transverse magnetic (TM) polarized (i.e., magnetic field normal to the plane of the periodicity of the PCs) and coupled into the input ridge waveguide (RW) using a  $40\times$  microscope objective lens. The light from the output RW was imaged onto an IR camera with another  $40\times$  objective lens, and the unwanted scattered light was blocked by irises. Using a thin-film 50/50 broadband (500 nm to  $1.8\ \mu\text{m}$ ) beam splitter, one-half of the output beam power was steered into an IR photodetector (New Focus Corp., Model No. 2033, bandwidth 0–30 kHz), which was connected to the input of the

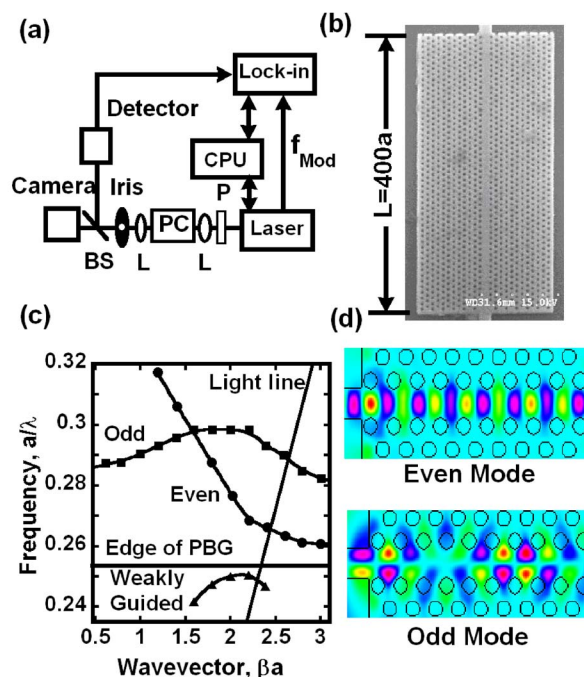


FIG. 1. (Color online) (a) Experimental setup schematic; (b) SEM picture of a 400-period triangular lattice W1 PCW, formed by removing one row of air holes, with input and output ridge waveguides: The radius of all holes is  $r=0.29a$ , where  $a=380$  nm is the lattice constant of photonic crystal. (c) Dispersion diagram of PCW calculated using the 3D FDTD method, in which filled circles represent even modes, filled squares represent odd modes and filled triangles represent weakly guided modes. (d) Simulated intensity profile of the even and odd modes of the PCW at normalized frequencies of  $a/\lambda=0.290$  and  $a/\lambda=0.295$ , respectively.

<sup>a)</sup>Electronic mail: jdhuang@ece.gatech.edu

lock-in amplifier. The lock-in amplifier was used to measure the power,  $R$ , of the output signal component having the same frequency as the reference signal from the input channel, and also to compare the phase shift,  $\Phi$ , between the output signal and the reference signal. This phase shift is a direct measure of the optical signal delay,  $\tau$ , with  $\Phi = 2\pi f_M \tau$ . The input laser wavelength was controlled by a computer, which iteratively recorded  $R$  and  $\Phi$ , for each selected wavelength.

The PCW samples were fabricated on a silicon-on-insulator wafer (Unibond wafer, from SOITEC Inc.). This wafer includes a Si slab of 260 nm thickness, which is separated from the Si substrate by a 1  $\mu\text{m}$  SiO<sub>2</sub> buried oxide layer. The thickness of the slab was chosen to ensure single-mode guiding along the normal direction of the wafer at wavelengths centered around 1.5  $\mu\text{m}$ . The PCWs were sandwiched between two RWs to couple light in and out the PCWs. The details of the manufacturing and sample preparation processes are published elsewhere.<sup>8</sup> The scanning electron microscopy (SEM) image of a typical sample, which features a 400-period triangular lattice of air holes (lattice constant  $a=380$  nm, hole radius  $r=0.29a$ ) is shown in Fig. 1(b). Samples of the same lattice structure with different lengths ( $L$ ) of  $50a$ ,  $100a$ , and  $150a$ , were used to better examine the properties of the PCWs.

We calculated the dispersion diagram and field profiles of the guided TM modes of the W1 PCW using a finite-difference time-domain (FDTD) technique by assuming an infinite thickness of the SiO<sub>2</sub> layer below the PCW structures. The results for the dispersion diagram and field profiles (i.e., intensity distribution) are shown in Figs. 1(c) and 1(d), respectively. The squares, circles, and triangles in Fig. 1(c) represent the odd, even, and weakly guided modes in this PCW, respectively. In the same figure, the light line of this PCW is plotted as the solid line, and the edge of the PBG is shown by the horizontal dotted line. The simulation results indicate that there exists a frequency range inside the PBG with no guided modes within the normalized frequency range  $0.25 < a/\lambda < 0.26$ , with  $\lambda$  being the light wavelength in a vacuum. We refer to such a frequency range as a photonic mode gap (PMG). At the same time, the light line crosses the even modes at the normalized frequency  $a/\lambda=0.265$ , above which only odd modes can be guided in this PCW. It is also seen from Fig. 1(d) that the power of the even mode is centered in the middle of the PCW, while the odd mode has almost zero intensity in that region.

In order to study the transmission properties of the PCWs, all transmission measurements were normalized to the transmission spectra of the reference RWs, i.e., transmitted power through the PCW structures is divided by that through a reference RW with the same width and total length fabricated on the same substrate. Figure 2(a) shows the transmission spectrum of a PCW with  $L=50a$ , from which a PMG can be clearly seen in the normalized frequency range  $0.24 < a/\lambda < 0.25$ . The signal group delay spectrum,  $\tau(\lambda)$ , can be directly deduced from the phase signal, which is measured simultaneously with the transmitted power using the lock-in amplifier. The results are plotted in Fig. 2(b): A group delay dip is clearly seen in frequency range of  $0.24 < a/\lambda < 0.25$  with a peak value of  $-0.86 \mu\text{s}$ , which corresponds to a phase value of  $-0.11$  rad (well above the system resolution of 0.017 rad). The frequency range of this group delay dip matches well with the PMG frequency range in the transmission spectrum in Fig. 2(a), which indicates the same physical origin, i.e., PMG, for these two features. This feature is similar to those observed in one-dimensional PC studies, where the PBG generates a group delay difference for various wavelengths.<sup>9</sup>

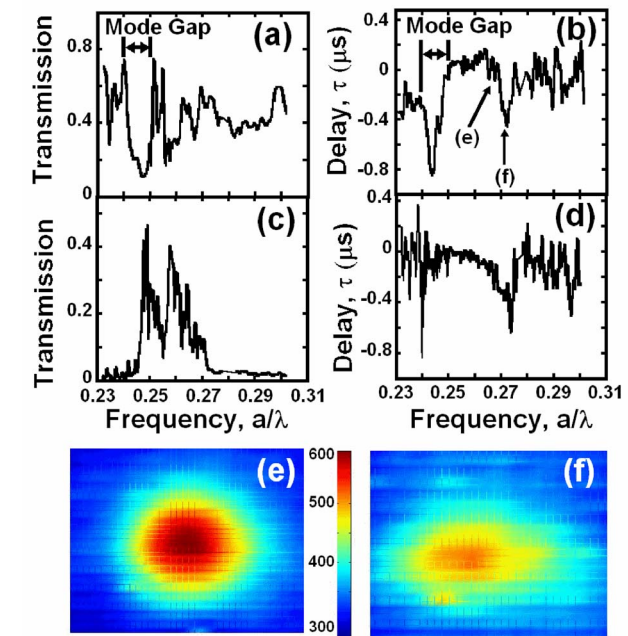


FIG. 2. (Color online) (a) Transmission and (b) signal group delay spectra of a 50-period triangular lattice photonic crystal waveguide (PCW). (c) Transmission and (d) group delay spectra of a 150-period triangular lattice PCW. Images in (e) and (f) are the far-field profiles corresponding to the frequencies marked in (b), respectively. The lattice constant of all the samples is 380 nm. Further properties of the photonic crystal structures are the same as those in the caption of Fig. 1.

An interesting deduction from the experimental data is that the optical signal travels at a speed of  $\sim 22$  m/s by simply taking into account the total length (19  $\mu\text{m}$ ) of the 50-period PC waveguides. This is almost four orders smaller than recently reported results.<sup>7,10</sup> We would like to mention one key difference between our method and those using an autocorrelator<sup>7</sup> or a near-field scanning optical microscope (NSOM):<sup>10</sup> The modulation frequency and the final bandwidth of the signal used in our measurements ( $\sim 0.8 \times 10^{-6}$  nm) are several orders of magnitude smaller than the bandwidth of a femtosecond pulse ( $\sim 20$  nm) used in those experiments, which allows us to measure much closer to the edge of the PMGs, where smaller group velocities are expected. We also observed significant distortion of the pulse shape at the extremely slow speed. At the same time, the ratio of delay over pulse duration is only 0.034, even at the delay peaks. A detailed discussion of the applications of these phenomena in slow light and optical transmissions is beyond the scope of this letter and will be published later.<sup>11</sup>

Aside from the above observations, we noted another group delay dip in frequency range of  $0.265 < a/\lambda < 0.274$  with a peak value of  $-0.48 \mu\text{s}$  [Fig. 2(b)]. There are no obvious features in the transmission spectrum [Fig. 2(a)], such as low transmission ranges, corresponding to this dip.

In order to confirm the generality of these observations, we measured the transmission and signal delay spectra of

we measured the transmission and signal delay spectra of

another PCW with the same lattice constant, but with  $L = 150a$ . The results are shown in Figs. 2(c) and 2(d). It is worth noting that compared with Figs. 2(a) and 2(b), the onset of the PMG in Figs. 2(c) and 2(d) is redshifted to  $a/\lambda = 0.245$  (for  $L = 150a$ ), as opposed to  $a/\lambda = 0.25$  (for  $L = 50a$ ) for both transmission and phase spectra. This small shift ( $\sim 2\%$ ) is likely the result of fabrication constraints. The PCW, which is now three times longer, has a very different transmission spectrum. A dramatic transmission reduction for frequencies below  $a/\lambda = 0.245$  and above  $a/\lambda = 0.265$  is observed for the longer structure. However, the group delay spectrum in Fig. 2(d) is very similar to that in Fig. 2(b): There is one dip peaked around  $a/\lambda = 0.24$  corresponding to the PMG, and another one peaked at  $a/\lambda = 0.272$ . Thus, the group delay spectra obtained by the lock-in technique are less sensitive to the length-induced loss and are therefore a powerful analytic tool for measuring the intrinsic properties of PC structures.

It is worth noting that the onset of high transmission (corresponding to the onset of the even mode) is at  $a/\lambda = 0.25$  in our experimental observations [Figs. 2(a) and 2(b)] as opposed to that at  $a/\lambda = 0.26$  in the simulation results [Fig. 1(c)]. This small difference ( $\sim 4\%$ ) between the numerical and experimental results likely comes from the assumption of infinite thickness of the  $\text{SiO}_2$  layer below the PC structures and other physical defects in the fabricated structure not accounted for in the simulations. Nevertheless, the numerical results can still provide qualitative insight if we shift the numerically simulated dispersion curves [Fig. 1(c)] down by  $a/\lambda = 0.01$ .

In the simulation results, the light line crosses the even modes at  $a/\lambda = 0.265$ , which is attributed to the small transmission dips in the experimental measurements at about  $a/\lambda = 0.255$  [Figs. 2(a) and 2(c)]. There are no guided modes (even or odd) between  $a/\lambda = 0.265$  and  $a/\lambda = 0.28$  below the light line. Above  $a/\lambda = 0.28$ , some odd modes below light line are allowed. In this sense, there is a parity change in the guided modes of the PCW. This mode parity change is attributed to the observed anomalous phase dip, which peaks around  $a/\lambda = 0.27$  as shown in Figs. 2(b) and 2(d).

In order to confirm this observation, we measured the far-field patterns corresponding to  $a/\lambda = 0.265$  and  $a/\lambda = 0.27$  [marked as (e) and (f) in Fig. 2(b), respectively]. The images are shown in Figs. 2(e) and 2(f), respectively. It is clear in these images that the far-field profile changes from a centered round mode to a more spread-out elliptical mode. It is worth noting that the signal power level at  $a/\lambda = 0.27$  is roughly the same as that at  $a/\lambda = 0.265$  [Fig. 2(a)], but the signal is delayed by about 400 ns compared to that at  $a/\lambda = 0.265$  [Fig. 2(b)]. A recent work using scanning near-field optical microscopy supports the claim of Bloch mode parity changes in these type of PCWs.<sup>12</sup>

Another interesting observation is that the odd modes in these PCWs exhibit much higher propagation losses as compared to the even modes. As shown in Figs. 2(a) and 2(c), the transmission peak around normalized frequency  $a/\lambda = 0.25$  (attributed to the even mode) is reduced by less than 3 dB as the PCW length ( $L$ ) increases from  $50a$  to  $150a$ . For the same length increase, the transmission around  $a/\lambda = 0.27$  (attributed to the odd mode) is reduced by almost 10 dB, adding proof to the claim of mode parity changes in this frequency range. The high loss of the odd modes might be due to the fact that the odd modes have their power concentrated on the edges of the guiding region of the PCWs, as shown in Fig. 1(d), and thus are sensitive to structural defects. The relatively slow group velocity measured at around  $a/\lambda = 0.27$  is a factor as well.<sup>13</sup>

In summary, we studied the transmission and group delay properties of triangular lattice PCWs using phase-sensitive lock-in techniques. In addition to the improved SNR for the transmission spectra measurements, we also observed large group delay dips at two specific frequencies, which are attributed to PMG and modal parity changes between the even and the odd modes. The experimental results demonstrate the power of the lock-in technique for the characterization of PC structures.

This work was supported by the Air Force Office of Scientific Research under contract no. F49620-03-1-062 (G. Pomrenke) and the National Science Foundation under contract no. ECS 0524255 (F. Bartolli). One of the authors (C.M.R.) would like to thank Lucent Technologies for support of his graduate studies.

<sup>1</sup>E. Yablonovitch, Phys. Rev. Lett. **58**, 2059 (1987).

<sup>2</sup>S. John, Phys. Rev. Lett. **58**, 2486 (1987).

<sup>3</sup>J. D. Joannopoulos, R. D. Meade, and J. N. Winn, *Photonic Crystals: Molding the Flow of Light* (Princeton University Press, Princeton, New Jersey, 1995).

<sup>4</sup>A. Chutinan, S. John, and O. Toader, Phys. Rev. Lett. **90**, 123901 (2003).

<sup>5</sup>N. Wu, M. Soltani, B. Momeni, M. Javanmard, A. Adibi, Y. Xu, and R. K. Lee, Opt. Express **11**, 1371 (2003).

<sup>6</sup>S. J. McNab, N. Moll, and Y. A. Vlasov, Opt. Express **11**, 2927 (2003).

<sup>7</sup>T. Asano, K. Kiyota, D. Kumamoto, B. Song, and S. Noda, Appl. Phys. Lett. **84**, 4690 (2004).

<sup>8</sup>A. Jafarpour, E. Chow, C. M. Reinke, J. Huang, A. Adibi, A. Grot, L. W. Mirkarimi, G. Girolami, R. K. Lee, and Y. Xu, Appl. Phys. B: Lasers Opt. **79**, 409 (2004).

<sup>9</sup>S. Wang, H. Erlig, H. R. Fetterman, E. Yablonovitch, V. Grubsky, D. S. Starodubov, and J. Feinberg, IEEE Microw. Guid. Wave Lett. **8**, 327 (1998).

<sup>10</sup>H. Gersen, T. J. Karle, R. J. P. Engelen, W. Bogaerts, J. P. Korterik, N. F. van Hulst, T. F. Krauss, and L. Kuipers, Phys. Rev. Lett. **94**, 073903 (2005).

<sup>11</sup>J. Huang, C. M. Reinke, A. Jafarpour, B. Momeni, M. Soltani, and A. Adibi (unpublished).

<sup>12</sup>B. Cluzel, D. Gérard, E. Picard, T. Charvolin, V. Calvo, E. Hadji, and F. de Fornel, Appl. Phys. Lett. **85**, 2682 (2004).

<sup>13</sup>S. Hughes, L. Ramunno, J. F. Young, and J. E. Sipe, Phys. Rev. Lett. **94**, 033903 (2005).